Application of the CESE Method to PDE Plume Dynamics Using a Beowulf Cluster

Hao He[1], Z.-C. Zhang[2], and S.-T. John Yu[3]
Mechanical Engineering Department,
Wayne State University, Detroit MI 48202
http://www.cfd.eng.wayne.edu/

Philip C. E. Jorgenson[4]
NASA Glenn Research Center
Cleveland, OH 44135
http://www.grc.nasa.gov/WWW/microbus/index.html

Abstract

In the present paper, we report high-fidelity CFD simulation of plume dynamics of a pulse detonation engine (PDE) by using modern parallel computer architecture. The two-dimensional axisymmetric Euler equations for reacting flows are solved by the Space-Time CESE method. A one-step global reaction is employed to model chemical reactions of a propane/air mixture. Computational domain includes the interior of the detonation tube and the aft quadrants of the PDE up to 12 feet in the axial direction and 4.5 feet in the radial direction. Numerical results of averaged pressures oscillation and the wave speeds compare well with the experimental data. For the required numerical resolution, we used a Beowulf cluster with the channel bonding. Our experience in using the system is summarized in the present paper.

1. Pulse Detonation Engine

Recently, Pulse Detonation Engine (PDE) [1-7] has attracted significant attention in propulsion research and development community. The PDE concept has the potential to improve vehicle performance and cost effectiveness over traditional air breathing propulsion devices for certain fly regimes. Figure 1.1 is a schematic of a typical PDE cycle of fueling, detonation initiation, and detonation blow down. Due to strong wave motions, acoustics has been a concern. In this paper, we used the Space-Time Conservation Element and Solution Element (CESE) method, to calculate the inherent wave motions and unsteady flow fields inside and outside of a PDE.

Pulsating jet noises of large amplitudes in both forward and aft quadrants are anticipated in flight tests of a PDE, in which a PDE will be integrated with a testing airplane. The amplitude and the propagation directions of pulsating plumes, and thus the resultant pressure loading on the fuselage and wings of the airplane, are of concern. The objective of the present paper is to perform high-fidelity simulation of plume dynamics, and to assess transient pressure loading in the vicinity of the thruster.

The computational problem here is challenging because the background mean flow is highly unsteady and with large vortex structures. Conventionally, computational aero acoustics for propulsion systems are performed in two steps: (1) CFD solutions of the RANS equations for the steady mean flows, and (2) the solution of a linear wave equation for the acoustic distribution.

In the present paper, this two-step approach is not applied due to the pulsating nature of the thrust plume. Instead, the highly accurate and efficient CESE method is employed to directly calculate the pulsating plumes for both mean flows and embedded acoustics.

2. The Model Equations

Consider the following Euler equations, coupled with a species equation:

PDE Cycle Summary

(1) ready for recharging

(2) fuel/air charging

(3) detonation initiated

(4) detonation wave propagating

(5) detonation wave at the exit
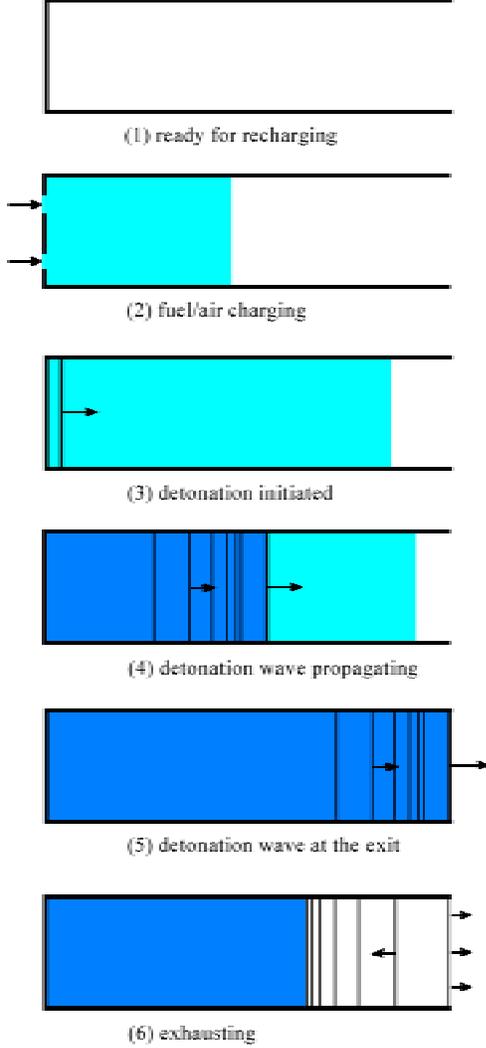
(6) exhausting

Fig. 1.1: A typical PDE cycle.

$$\frac{\partial \mathbf{U}}{\partial t} + \frac{\partial \mathbf{F}}{\partial x} + \frac{\partial \mathbf{G}}{\partial y} = \mathbf{R}. \qquad (2.1)$$

where the vector $\mathbf{U}$ is the unknown, $\mathbf{F}$ and $\mathbf{G}$ are flux vectors, and $\mathbf{R}$ is the source term vector. Each vector has five entries for the continuity, two moments, the energy, and the species equations:

$$\mathbf{U} = \begin{pmatrix} \rho \\ \rho u \\ \rho v \\ \rho E \\ \rho Z \end{pmatrix}, \ \mathbf{F} = \begin{pmatrix} \rho u \\ \rho u^2 + p \\ \rho uv \\ (\rho E + p)u \\ \rho uZ \end{pmatrix}, \ \mathbf{G} = \begin{pmatrix} \rho v \\ \rho uv \\ \rho v^2 + p \\ (\rho E + p)v \\ \rho vZ \end{pmatrix},$$

$$\mathbf{R} = \begin{pmatrix} -\rho v / y \\ -\rho uv / y \\ -\rho v^2 / y \\ -(\rho E + p)v / y \\ -\rho vZ / y + \dot{\omega} \end{pmatrix}. \qquad (2.2)$$

Here, ρ is density, u, v are the x-, y- components of velocity, p is pressure, Z is the mass fraction of the reactant, and $E = e + Zq_o + (u^2 + v^2)/2$ is the total energy with e as the internal energy and q_o as the heat release due to the chemical reaction. In the species equation, a source term exists due to a one-step, irreversible chemical reaction, which is modeled by finite-rate kinetics:

$$\dot{\omega} = -K\rho Z \exp(-E^+ / R_u T), \qquad (2.3)$$

where K the Arrhenius coefficient, E^+ is the activation energy, and R_u is the universal gas constant. The gas mixture is assumed to be polytropic, i.e., the molecular weights and the specific heats are constant for both unburned and burned gases. The above equations are nondimensionalized based on the half reaction length scale and time scale of the detonation wave. For details, refer to our previous works for detonations [13-16].

3. The CESE Method

Originally developed by Chang and coworkers, the CESE method [8-12] is a new numerical framework for conservation laws. The CESE method employs a unified treatment for space and time to enforce local and global space-time flux conservation, which differs substantially from conventional CFD methods. No Riemann solver or reconstruction procedure is used, and the use of a priori knowledge of the solution, such as total variation diminishing, which is not true for reacting flows, is completely avoided, yet the capabilities of the CESE method in capturing shock waves, contact discontinuities, and shedding vortices are superb. Moreover, the CESE method is a true multi-dimensional CFD scheme. No directional splitting is used to calculate spatial fluxes and source terms. To date, numerous flow problems involving complex wave motions and interacting vortices have been solved by the one-, two-, and three-dimensional Euler and Navier Stokes CESE solvers using both structured and unstructured meshes for flows at all speeds.

4. Parallel Computing

A Beowulf computer system is used to calculate the PDE plumes. The system is a cluster of PCs interconnected by high-speed networks. These PCs run an open-source UNIX operating system, e.g., Linux and Free BSD. Parallel application programs are executed using industry standard message passing models and libraries, e.g., MPI. As a typical example of a low-cost Beowulf cluster, our cluster is illustrated in Figs. 4.1 and 4.2.

To perform parallel computation, we split computational tasks into parallel tasks by using message passing, network sockets, and/or inter-process communication (IPC). Software systems, e.g., MPI and PVM, allow us to write message-passing parallel programs, which run on a cluster. The application programs could be written in Fortran, C, and C++. MPI is a library of functions and macros that can be called by our application programs for communication between computer nodes. MPICH, a popular MPI implementation, is used in our cluster.
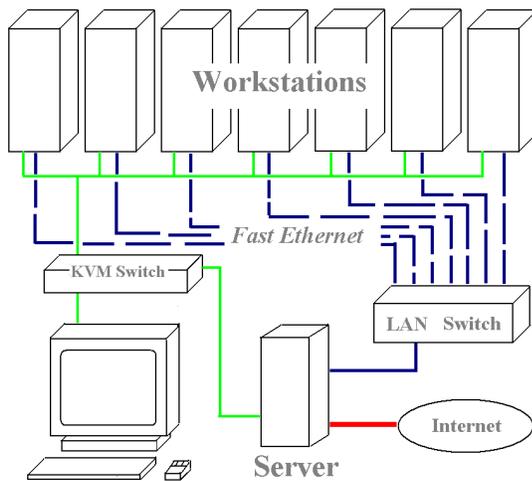

Fig. 4.1: A schematic of a Beowulf cluster.

Effective use of a Beowulf system requires a proper distribution of simulation tasks among the available processing nodes. A common approach is to decompose the computational domain into a number of partitions, and to assign the partitions to different nodes. The processing nodes execute the same CFD solver but in different sub-domains. They communicate to exchange intermediate numerical results at sub-domain boundaries at the end of each time step. A proper domain decomposition would balance the computational workload and memory occupancy of processing

nodes, while minimizing the inter-node communication.

Fig. 4.2: Timesurfer (a Beowulf cluster) at Wayne State CFD group.

To improve the performance of Beowulf systems, one needs to employ fast processors, fast memories with large bandwidth, fast network components, and in some cases, fast hard drives. Intel and AMD processors with frequency up to 2 GHz provide powerful computation capacity. RDRAM and DDR SDRAM memories provide up to 3200 MB/s bandwidth to match the speed of

modern powerful processors. However, without fast networks, fast processors and memory systems are useless to a Beowulf cluster. High-speed communication among computer nodes is imperative. Currently we are using 100M Fast Ethernet LAN. Gigabit switches and the associated Ethernet products are also available. However, the cost is considerably higher. With the support to channel-bonding technology in recent Linux kernel, we can 'bond' multiple Ethernet interfaces into a faster 'virtual' Ethernet interface to get higher data transmission speed.

Fig. 4.3: A schematic of channel bonding with dual fast Ethernet NIC (network interface card).

To proceed, we illustrate the following test of Channel Bonding performance based on systems equipped with multiple 3C905B NIC and 2.4 kernel Linux operating system, benchmarked by Netperf 2.1. The maximum data transfer rates are 94.1 Mbps, 188.2 Mbps, 278.6 Mbps in 1 NIC, 2 NIC, 3 NIC case, respectively. When 4 NIC are used, the performance is worse than 3 NIC, because of the limited bandwidth of PCI bus. It is remarkable that 3 NIC systems out perform systems using Gigabit technology.

The test result shows that if the size of the messages exchanged among the nodes is less than 100 bytes, the performance difference between a 1-NIC system and multi-NIC system is minimum. When the message size exceeds 100K bytes, 3 NIC systems reach its peak data transfer rate. According to our experience, in two- and three-dimensional CFD, the message size is about 1KB to 500KB. Note that bonding Gigabit cards cannot bring expected performance at this time. The 32-bit PCI bus cannot handle multiple 64-bit Gigabit cards.
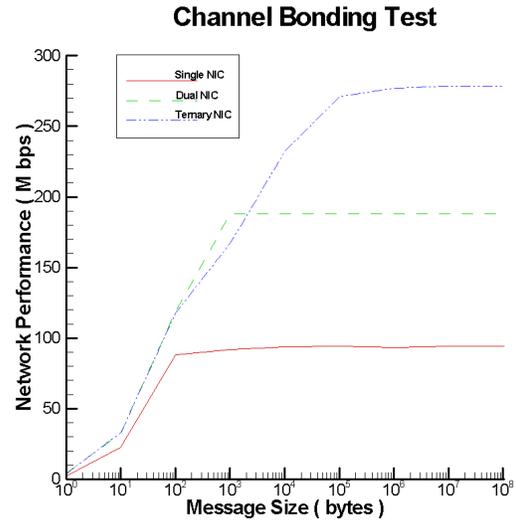

Fig. 4.4: Network bandwidth test in Channel Bonding.

Table 4.1: Web Sites of Beowulf Cluster.

www.beowulf.org	Software, documentation, papers for Beowulf clusters, and links to other resources and cluster sites. Hosted by Scyld Computing corp.
www.scyld.com	Scyld Computing corp., Linux Beowulf clusters developer.
www.linux.org	Linux Online
www.linuxdoc.org	Linux Documentation Project
www.cs.berkeley.edu/ ~mdw/linux/hpc/hpc. html	Linux in High Performance Computing
www-unix. mcs.anl.gov/ mpi/	MPI introduction and MPICH's home page
www-users.cs.umn.edu/~ka rypis/metis/	METIS's home page METIS provides a fast and high-quality multilevel scheme for partitioning irregular domains.

4

To get good performance in parallel computing, the following key requirements must be met: (1) well-organized fast network, (2) balance in decomposition of calculating domain, and (3) effective communication function call in parallel programming. Table 4.1 lists several web sites for useful information.

5. Numerical Results

We apply our Beowulf system to simulate the two-dimensional PDE plume. Premixed gas mixture of fuel and air burns inside the PDE chamber, and detonation waves travel through the thrust tube and exit to the ambient atmosphere. The flow field outside of the PDE tube is to be investigated. The numerical results at specific locations are recorded and compared with experimental data.
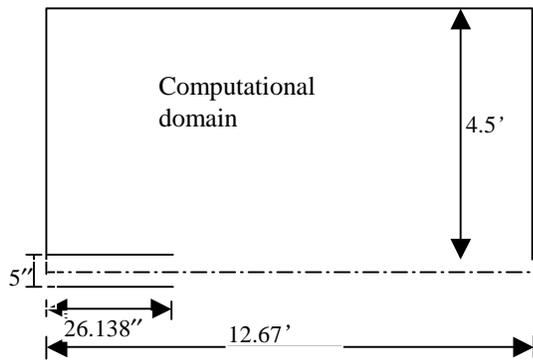

Fig. 5.1: The schematic of computational domain for a single tube and single firing condition.
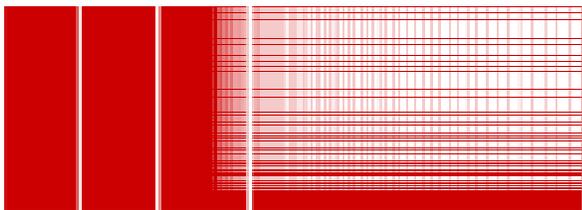

Fig.5.2: The schematic of mesh decomposition in PDE simulations.

Figure 5.1 shows the computational domain of a single tube thruster. The radius of the tube is 5 inches, and its length is 26.138 inches. Due to the flow symmetry, the region above the central line is the computational domain. The length and radius of the computational domain are 12.67 ft and 4.5 ft, respectively. Current mesh contains 290,360

rectangular cells. Inside and near thrust tube, the mesh contains fine uniform cells. The mesh stretches to be with large-size cells at far boundary. Figure 5.2 shows the mesh employed. Four domains are used for parallel computation in this case. The domain decomposition is straightforward due to the simple geometry.

To examine the details of the complex flow, we recorded time histories of pressure and density at 36 checking points. These numerical data are compared with NASA's experimental data. As shown in Fig. 5.3, all checking points are distributed on a plane below and parallel to the symmetric line with a distance of 5 7/8 inches. The 36 checking points are divided to four sets, located along four lines on the plane, i.e., L-1, L-2, L-3, and L-4. The L-1 line is the projection of the thrust vector (or the symmetric line) to the checking-point plane, and the origin is corresponding to the PDE tube exit on the symmetric line. Ten checking points are distributed along L-1 with distances from origin at the testing plane of 4, 5.66, 8, 11.32, 16, 22.64, 32, 45.28, 64, 90.56 inches. Checking points on L-2, L-3 and L-4 are the corresponding ones rotated counterclockwise from L-1 at angles of 30º, 60º, and 90º, respectively. Note that there are only 8 checking points on L-3 and L-4. Since the axisymmetric Euler equations are solved, we must map all checking points to the computational domain by using the Pythagoras theorem. Refer to the triangle in Fig. 5.3. In the mapping, we simply use the numerical solutions at the grid points closest to the checking points.
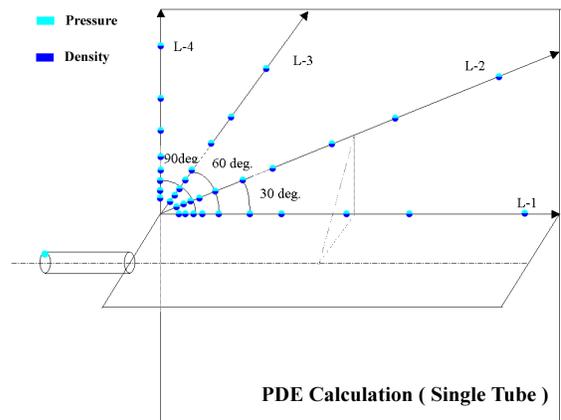

Fig. 5.3: Checking points distribution.

At the beginning of each firing, 85% of the tube is filled with a propane/air mixture at a fuel/air ratio $\Phi=1.3$. The initial chamber pressure is 15.0 psia,

and temperature is 510 R. The C-J detonation velocity $V_{C\text{-}J}$=6200ft/sec., shock pressure jump P_2/P_1=16.667. The PDE tube operates at 60 Hz, i.e., 16.67 ms for one cycle. When t=0, the initial detonation wave is located at H_1, which is 1.04 cm from the closed end. Refer to Fig. 5.4. For the initial condition, the ZND analytical solution [13] is mapped to eight mesh nodes along central line at the closed end.
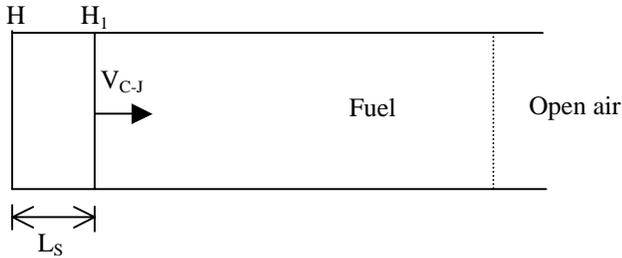

Fig.5.4: Initial condition.

The parameters for one-dimensional analytical solution are determined by running the CEA program [17] with the experimental condition as input data. The output data from CEA program are also compared with experimental data for checking consistence. In the setting of the model equation employed, the detonation wave can be specified by four parameters, i.e., γ, q_0, f and E^+, where f is overdriven factor. In the present calculation, the Chapman-Jouguet (C-J) detonation is anticipated, therefore f=1.

For the specific hear ratio, the CEA program showed $\gamma = 1.2013$ for the burned gases. T_0 and $V_{C\text{-}J}$ given in the experimental data, with the value of Cp from results of CEA program, i.e., Cp=2.1064, we can obtain D_{C-J} =5.974, which is non-dimensionalized by the speed of sound of the unburned gases. With γ and $D_{C\text{-}J}$ known, we can employ classical C-J velocity equation and obtain $q_0 = 37.563$. Parameters E^+ and $L_{1/2}$ (or K) depend on the reaction rate, and determine the width of reaction zone. These two parameters can only be determined by experiments. Based on the prescribed mesh spacing, we use E^+ =35. Due to the length limit of the AIAA papers, the above description of the controlling parameters is brief and incomplete. We are in the process of compiling a comprehensive report for the present calculation, which will be available through NASA Glenn.

The detonation wave is ignited at the closed end of the thrust tube, and travels from left to right. Figure 5.5 shows the time history of pressure at the

closed end of the thrust tube for a single pulse firing. At ignition, pressure jumps up to more then 17 bars, which is the equilibrium C-J pressure of a propane/air detonation. After a very short period of time, pressure at the closed end quickly drops to about 6.5 bars due to the induced flow expansion behind the traveling detonation wave. The time before the pressure at the closed end starts to drop is about 0.9 ms. This is the time when the PDE tube produces thrust forces. Pressure declines steeply after the expansion wave has reached the closed end of the PDE tube. From 3.4 ms to about 10 ms, the closed-end pressure oscillates and approaches the atmospheric level gradually. These pressure fluctuations are the result of complex vortex/shock interactions outside the detonation tube, and they are detrimental to the refueling and purging processes.
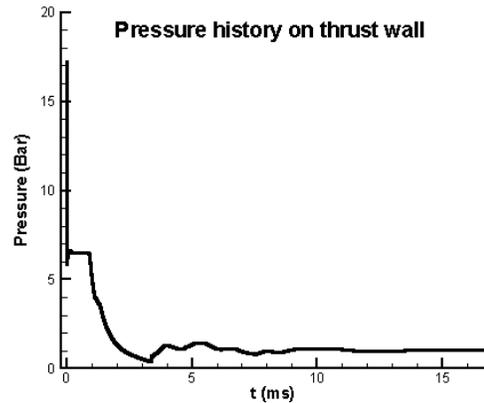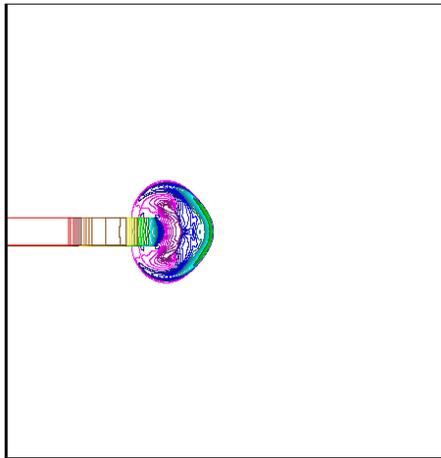

Fig. 5.5: Time history of pressure at the closed end of a propane/air thrust tube single pulse firing condition.
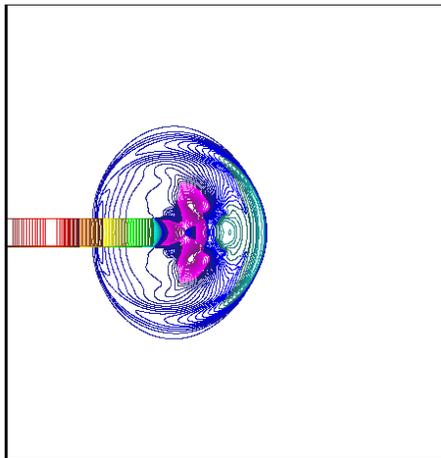
Figure 5.6 shows three snapshots of the pressure contours after the detonation wave has left the thrust tube. The detonation wave quickly quenches and becomes a spherical pressure wave, which is identical to the wave expansion model proposed by Wilson and Paxson [6].

Time histories of pressures at all checking points show similar pattern, i.e., one pressure peak followed by a trough and subsequent minor oscillations. Away from the PDE tube exit, the pressure peaks and troughs are more gradual. Figure 5.7 shows pressure histories at two checking points.
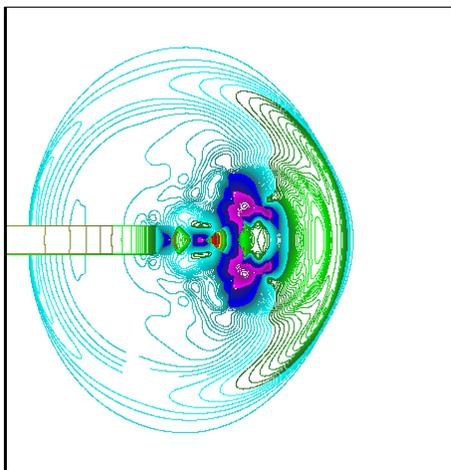
Peak pressures and their corresponding times for the PDE wave passing all checking points are shown in Fig. 5.8(a). The experimental data on L-1 is also included. Our numerical results compare favorably with the experimental data.
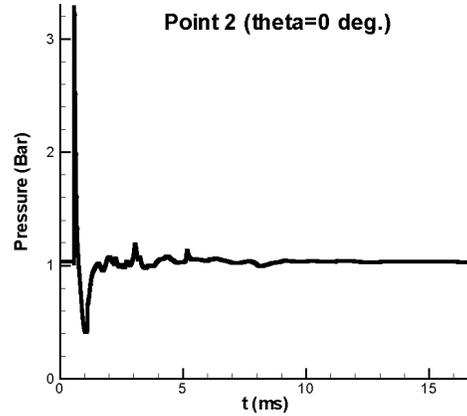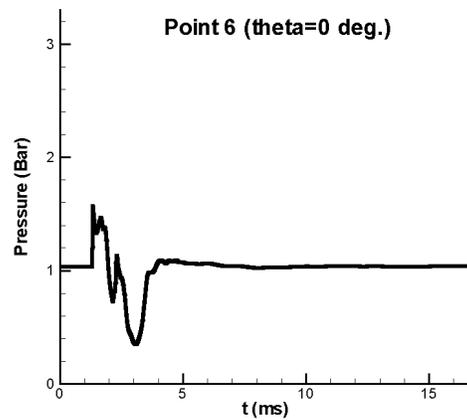
6

(a) $t = 0.642\ ms$

(b) $t = 1.124\ ms$

(c) $t = 1.927\ ms$

Fig 5.6: Three snapshots of pressure contours of a PDE plume at the initial stage of expansion.
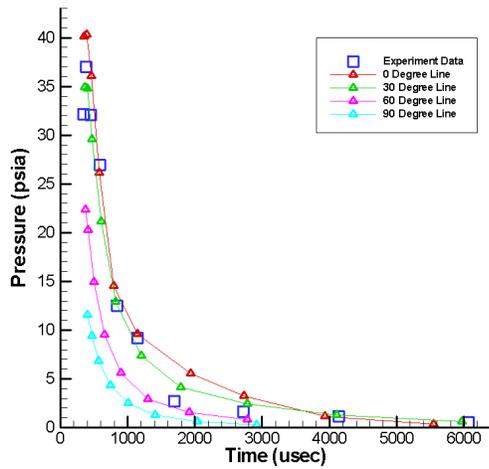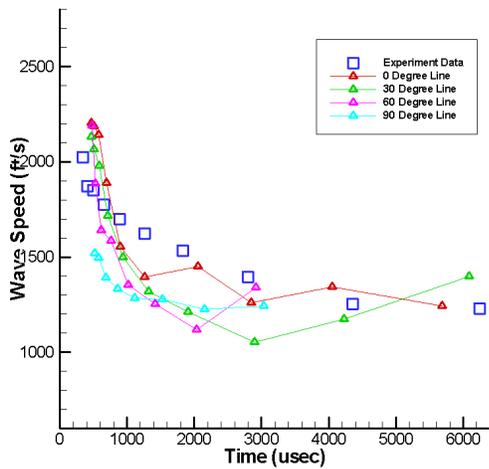

(a)

(b)

Fig. 5.7: Time histories of pressures at two checking points with the locations at (a) (5.66", 5.875") and (b) (22.64", 5.875").

The wave speeds of the pressure peaks and troughs are also checked and compared with the experimental data. Refer to Fig. 5.8(b). To calculate the wave velocity, we perform numerical interpolation of the times of pressure peaks at a group of mesh nodes in the vicinity of the checking points.

Once out of the PDE tube, the hot burned gases quench and the associated wave speeds decrease accordingly. Note that the wave speed at the first checking point, which is only 7.11 inches away from the PDE exit, is about 2,200 ft/sec. However the C-J detonation speed is over 6,000 ft/sec inside the PDE chamber. The shock wave experiences tremendous quenching and thus slow-down in a very short distance.

by complex vortex structure in the PDE plume. In a pervious paper, we have shown that the PDE plume in the near field is dominated by shock-vortex interactions [14]. Moreover, numerical calculations were performed based on the assumption that the ambient atmosphere is clean and at the specified initial condition, which may not be true for the testing environment after several testing firings.

(a)

(b)

Fig. 5.9: (a) Peak pressures and (b) wave speeds at checking points along L-1 for the initial chamber pressure at 18.5 psia.
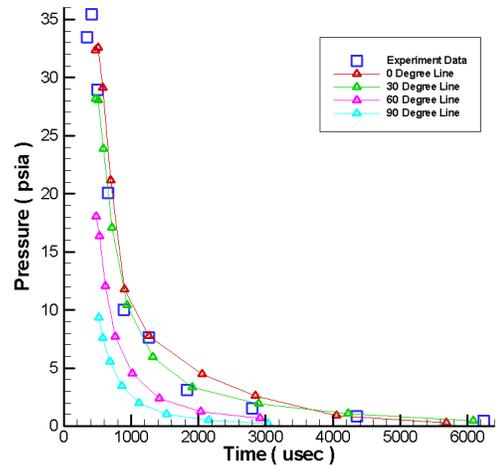

(a)

(b)

Fig. 5.8: (a) Peak pressures and (b) wave speeds at checking points along L-1 for the initial chamber pressure at 15.0 psia.
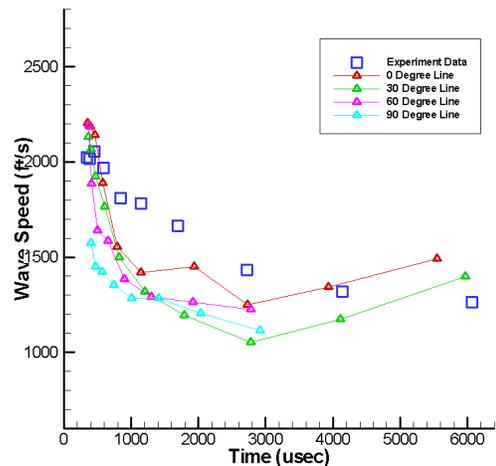
Figure 5.9 shows results for a different testing condition. As compared to the case in Fig. 5.8, the chamber pressure here is 18.5 psia. All other initial conditions are identical to that in the previous case. After equilibrium calculation using the CEA program, the controlling parameters of the present detonation are f =1.0, γ=1.2049, $q_o = 37.183$, $E^+=$ 35, respectively.

Unlike the experimental results, the decay of the wave speeds predicted by the CFD calculation is not monotonic. Instead, significant fluctuations of wave speeds can be discerned. This may be caused

6. Concluding Remarks

In the paper, we report our experience of developing and using a Beowulf cluster computer to perform CFD calculations of PDE plumes. Key points to improve the performance of Beowulf systems are discussed. Detailed numerical results of axisymmetric PDE plumes are reported. Comparison with available experimental data is presented. The result shows that the CESE method is a highly accurate and efficient method for this particular CAA problem. The synergy of this novel numerical method and the cost-effective parallel computation could point to a new direction for high performance computing for unsteady flows relevant to advanced propulsion systems. Please refer to our web site http://www.cfd.eng.wayne.edu for more information about our efforts in applying the CESE method to various engineering thermal–fluid problems.

References

1. K. Kailasanath, G. Patnaik and C. Li, "Computational Studies of Pulse Detonation Engines: A Status Report," AIAA 99-2634 (1999).

2. C.P. Li, K. Kailasanath and G. Patnaik, "A Numericaal Study of Flow Field Evolution in a Pulsed Detonation Engine," AIAA paper 2000-0314 (2000).

3. K. Kailasanath, "A Review of PDE Research: Performance Estimates," AIAA paper 2001-0474 (2001).

4. H.B. Ebrahimi, R. Mohanraj, and C.L. Merkle, "Multi-Level Analysis of Pulse Detonation Engine," AIAA Paper, 2000-3589 (2000).

5. F. Schauer, J. Stutrud, and R. Bradley, "Detonation Initiation Studies and Performance Results for Pulse Detonation Engine Applications," AIAA Paper 2001-1129 (2001).

6. J. Wilson and D. E. Paxson, "On the Exit Boundary Condition for One-dimensional Calculations of Pulsed Detonation Engine Performance," the 18th International Colloquium on the Dynamics of Explosions and Reactive Systems, July 29th -August 3, 2001, Seattle, Washington.

7. T. E. Bratkovich, M. J. Aarnio, J. T. Williams and T. R. A. Bussing, "An Introduction to Pulse Detonation Rocket Engines (PDREs)", AIAA paper 97-2742 (1997).

8. S. C. Chang, The Method of Space-Time Conservation Element and Solution Element – A New Approach for Solving the Navier Stokes and Euler Equations, *J. Comput. Phys*., 119 (1995) p. 295

9. S.C. Chang, X.Y. Wang and C.Y. Chow, The Space-Time Conservation Element and Solution Element Method: A New High-Resolution and Genuinely Multidimensional Paradigm for Solving Conservation Laws, *J. Comput. Phys.,* 156 (1999) p. 89.

10. S. C. Chang, X. Y. Wang and W. M. To, "Application of the Space-Time Conservation Element and Solution Element Method to One-Dimensional Convection-diffusion Problems," *J. Comput. Phys.,* 165, 189 (2000).

11. S.C. Chang, A. Himansu, C. Y. Loh, X. Y. Wang, S.T. Yu, P. Jorgenson, Robust and Simple Nonreflecting Boundary Conditions for the Space-Time Conservation Element and Solution Element Method, AIAA Paper 97-2077 (1997).

12. S.T. Yu and S.C. Chang, "Treatments of Stiff Source Terms in Conservation Laws by the Method of Space-Time Conservation Element and Solution Element," AIAA Paper 97-0435 (1997).

13. Z.C. Zhang, S.T.J. Yu, H. He, S.C. Chang, "Direct Calculations of Two- and Three-Dimensional Detonations by an Extended CESE Method," AIAA Paper 2001-0476 (2001).

14. Z.C. Zhang, S.T.J. Yu, H. He, P.C.E. Jorgenson, "Direct Calculations of Plume Dynamics of a Puls Detonation Engine by the Space-Time CESE Method", AIAA Paper 2001-3614 (2001)

15. S.J. Park, S.T. Yu, M.C. Lai, S.C. Chang,and P.C.E. Jorgenson, "Direct Calculations of Stable and Unstable ZND Detonations by the Space-Time CESE method," AIAA Paper 98-3212 (1998).

16. H. He, Z.C. Zhang, S.T.J. Yu, S.C. Chang, "Three-Dimensional Simulations of Detonations by the CESE Method Using a

Low-Cost Beowulf Cluster", AIAA Paper 2001-0140 (2001).

17. B. J. McBride and S. Gordon, "Computer Program for Calculation of Complex Equilibrium Compositions and Applications," NASA Reference Publication 1311, NASA Lewis Research Center (1996).